

# Growth and Structure of water on SiO<sub>2</sub> films on Si investigated by Kelvin probe microscopy and in situ X-ray Spectroscopies

*Albert Verdaguer<sup>1,3</sup>, Christoph Weis<sup>1</sup>, Gerard Oncins<sup>4</sup>, Guido Ketteler<sup>1</sup>, Hendrik Bluhm<sup>2</sup> and Miquel Salmeron<sup>1\*</sup>*

<sup>1</sup>Materials Sciences Division and <sup>2</sup>Chemical Sciences Division

Lawrence Berkeley National Laboratory

University of California, Berkeley, California 94720. USA

<sup>3</sup>Institut Català de Nanotecnologia (ICN)

Campus de Bellaterra-Facultat de Ciències, Edifici C-Ala Nord-Mòduls, 08193 Bellaterra, Spain

<sup>4</sup> Department of Physical Chemistry, Universitat de Barcelona, 08028 Barcelona, Spain

E-mail: mbsalmeron@lbl.gov

The growth of water on thin SiO<sub>2</sub> films on Si wafers at vapor pressures between 1.5 and 4 torr and temperatures between -10 and 21°C has been studied *in situ* using Kelvin Probe Microscopy and X-ray photoemission and absorption spectroscopies. From 0 to 75% relative humidity (RH) water adsorbs forming a uniform film 4-5 layers thick. The surface potential increases in that RH range by about 400 mV and remains constant upon further increase of the RH. Above 75% RH the water film grows rapidly, reaching 6-7 monolayers at around 90% RH and forming a macroscopic drop near 100%. The O K-edge near-edge X-ray absorption spectrum around 75% RH is similar to that of liquid water (imperfect H-bonding coordination) at temperatures above 0 °C and ice-like below 0 °C.

## Introduction

At ambient conditions all materials on earth are exposed to water vapor that produces films on their surfaces. The thickness and structure of this film is determined by the interaction forces between the surface and the adsorbed water molecules and has important implications for industrial, environmental and biological processes. One fundamental question is the range of the surface-induced modifications, if any, of the structure of water. In other words, how many layers are needed for water to reach its bulk structure? Not surprisingly the study of water at interfaces is a very active field, as demonstrated by the numerous review articles on this topic published in recent years.<sup>1-4</sup>

Oxide surfaces are particularly important and have received considerable attention.<sup>5</sup> One of the most important oxides is amorphous SiO<sub>2</sub> because of its widespread presence in silicon technology and in natural minerals.<sup>6-8</sup> The surface of amorphous SiO<sub>2</sub> is usually modeled by a mixture of the (111) and (100) surfaces of hydroxylated  $\beta$ -cristobalite, which expose single and geminal hydroxyl groups, respectively.<sup>9</sup> On a fully hydroxylated (100) surface these groups are sufficiently close to each other that H-bonded networks can be formed. In the (111) surface the hydroxyl groups are more separated so that no H-bonds can form between them.

The structure of water in contact with different SiO<sub>2</sub> surfaces has been studied both theoretically<sup>10-13</sup> and experimentally<sup>14-18</sup>. These studies have predicted an ordered hexagonal water layer on the hydroxylated surface of quartz (0001)<sup>13</sup> and a hexagonal ice-like structure on a fully hydroxylated  $\beta$ -cristobalite (100) surface.<sup>10</sup> However there is some controversy about the stability of such monolayer structures at room temperature.<sup>12</sup> No ice-like structure has been predicted for cristobalite (111) and the most favorable site for water molecules has been predicted to be a hollow site with the molecules forming 2 or 3 H-bonds with surface silanol groups.<sup>11</sup> Based on optical experiments an ice-like monolayer on amorphous SiO<sub>2</sub> has been proposed at room temperature and 10% relative humidity (RH).<sup>14</sup> Information on the structure of water films thicker than a monolayer is much scarcer. Sum-frequency vibrational spectroscopy experiments have shown a mixture of ice-like and water-like structures on the surface of quartz (0001) immersed in water.<sup>17</sup> Infrared (IR) experiments have been

performed to study the growth of water on amorphous SiO<sub>2</sub>.<sup>15</sup> Different features of the spectra were assigned to ice-like and liquid-like water and were used by the authors to suggest an ice-like growth of the water film up to 3-4 monolayers, followed by a liquid water film above that.

In this paper we present the results of a study of the growth and structure of water on SiO<sub>2</sub> by several techniques, namely surface potential measurements using an atomic force microscope (AFM), ambient pressure X-ray photoemission and near-edge X-ray absorption fine structure spectroscopies (XPS and NEXAFS). Our studies using these various techniques indicate that above 0°C about 4 water layers are sufficient for the water molecules to reach a structure similar to that of a thick water film.

## **Experimental section**

**Sample preparation:** Silicon (111) wafers were ultrasonically cleaned in acetone and methanol for about 10 min. Organic contamination and the native oxide layer were removed using the RCA standard cleaning method.<sup>19</sup> A new oxide layer was then grown by exposing the surface to UV/O<sub>3</sub> for 45 min, followed by rinsing with Millipore water and drying with nitrogen. Recent studies have shown that this UV/O<sub>3</sub> treatment promotes the growth of a clean, high quality oxide layer.<sup>20,21</sup> On surfaces prepared in this way a small drop of water spread forming a film with a contact angle very close to zero.

**AFM experiments:** Contact potential differences between the AFM tip and the sample were measured at room temperature ( $21 \pm 1^\circ\text{C}$ ) on a home-built AFM<sup>22</sup> and with an electronic controller from RHK<sup>23</sup>. The microscope was enclosed in a glove box where humidity could be controlled by circulating either dry or wet N<sub>2</sub> (bubbling through Millipore water). The relative humidity (RH) was measured using an Omega hygrometer with accuracy of  $\pm 5\%$ . The AFM was operated in the Scanning Polarization Force Microscopy (SPFM)<sup>24</sup> mode. Using this mode we could measure the sample topography in non-contact mode while simultaneously recording maps of the local contact potential difference (Kelvin Probe Mode),<sup>25</sup> where the amplitude of the first harmonic of the lever oscillation due to the electrostatic force is nulled by a feedback bias voltage. We used Pt-coated tips functionalized with alkylthiols that render them hydrophobic. This was necessary to prevent adsorption of water on the tip and avoid changes of

the tip work function during the experiment. In this manner changes in contact potential difference are interpreted as changes in the surface potential of the sample.

XPS experiments: The thickness of the water film on the SiO<sub>2</sub> surface was measured using XPS in a chamber that could be pumped, baked and annealed to achieve pressures of  $\sim 10^{-10}$  Torr previous to the introduction of water vapor. In addition to measuring the thickness of the surface films, XPS provides also information on the oxidation state of the substrate and its cleanliness. The measurements were performed at beamline 11.0.2 of the Advanced Light Source (ALS) at Lawrence Berkeley National Laboratory using a photoelectron spectrometer that can operate at pressures of up to a few Torr. As described previously<sup>26</sup> it consists of a chamber with a differentially pumped electrostatic lens system that focuses the electrons emitted by the sample into the focal plane of a hemispherical electron energy analyser. Photoemission spectra of the Si2p and O1s core levels were recorded using incident photon energies of 290eV and 720eV, respectively. In this way photoelectrons from the Si2p and O1s core levels have similar kinetic energies ( $\sim 190$  eV), which ensures that the probing depth is similar in all recorded spectra. The sample position was changed between the acquisition of spectra to minimize beam damage and further oxidation of the substrate by reaction with OH-groups that might be formed activated by the incident photons.<sup>2</sup> The possible growth of the oxide film was monitored by checking the ratio of SiO<sub>2</sub> to elemental Si peaks (Si2p(Si<sup>4+</sup>)/Si2p(Si<sup>0</sup>)) at the same location while acquiring spectra, and found to be negligible. The binding energy scale in all experiments was calibrated using the known value for the elemental Si2p<sub>3/2</sub> peak (99.4 eV) as a reference.<sup>27</sup>

The XPS peaks were deconvoluted by Gauss-Lorentz profiles after subtraction of a linear background and normalized by the incident photon flux and energy-dependent X-ray absorption cross sections.<sup>28</sup> Since the O1s region contains overlapping contributions from oxygen atoms in the silicon oxide and in the adsorbed water, the water contribution was obtained by subtracting the peak due to the oxide from the spectra. To that effect first the peak shape of the silicon oxide O1s peak and the normalized Si2p(Si<sup>4+</sup>)/O1s peak ratio was determined on a dry sample (Fig. 1a). Then, in the presence of adsorbed water, the O1s intensity due to the oxide substrate was calculated from the measured Si2p(Si<sup>4+</sup>) peak

intensity. The O1s spectra were fitted using three peaks, one for the gas phase water, one constrained to the calculated silicon oxide peak intensity (from the Si2p(Si<sup>4</sup>) intensity), using the line shape determined under dry conditions, and the third for the remaining intensity, which is assigned to the adsorbed water film (fig. 1b). Differences in attenuation of the signal intensity by the gas phase were accounted for by plotting the relative O1s(H<sub>2</sub>O<sub>adsorbed</sub>)/Si2p(SiO<sub>2</sub>) ratio. The thickness of the oxide layer was calculated following the method of Himpsel et al.<sup>29</sup> and found to be 2.4±0.2 nm, with the error indicating statistical dispersion. This method can also be used to calculate the thickness of adsorbed layers on SiO<sub>2</sub> surfaces such as water and carbon contamination<sup>21</sup>. To calculate the amount of adsorbed water we used an electron mean free path through the water film of 1.5 nm at the 200 eV kinetic energy used here.<sup>30</sup> Typically the initial carbon contamination was about one tenth of a monolayer, but increased as water was introduced in the chamber, reaching a maximum of ~1/2 monolayer in one of the experiments. After water was introduced contamination only showed slight variations throughout the RH increase. No effects due to this small amount of contamination could be discerned.

NEXAFS experiments: NEXAFS spectra were obtained by collecting O KLL Auger electrons (kinetic energy 465-485 eV), which have a mean free path of ~2 nm in water and thus reflect the properties of the first few surface layers. The raw data contain contributions from the gas phase and from the oxide substrate, which have to be removed to obtain spectra of only the water film. The pure gas phase spectrum was obtained by using a hydrophobic graphite (HOPG) crystal placed at the same position as the SiO<sub>2</sub>/Si sample and measured under identical background water vapor pressures as in the H<sub>2</sub>O/SiO<sub>2</sub> experiments at very low humidity (~5% RH). The substrate oxide contribution was determined by measuring the SiO<sub>2</sub> films under vacuum at very low humidity conditions. These procedures are described in detail in the supporting information section.

Isotherms and isobars: While the AFM experiments were purely isothermal those in the photoelectron spectroscopy chamber were not, due to the limited upper pressure of 4 torr achievable. To reach high humidity in that case the sample was cooled, so that the experiments were in the form of isobars. Different experiments were performed at 1.5, 3 and 4 torr of water vapor pressure. Only in a few

experiments in that chamber high humidity was reached by increasing the water vapor pressure by keeping sample temperature constant. The RH value was then obtained by dividing the vapor pressure by the saturation vapor pressure *at the sample temperature*. Although the vapor is at room temperature while the sample is not, the error incurred by this procedure is negligible. This is due to the fact that equilibrium is determined by the equality of the rate of adsorption of gas molecules on the surface, which varies as  $p/\sqrt{T}$ , and the rate of desorption, which varies as  $\exp(-E/kT)$ . It is clear that it is the surface temperature that is by far the most important and the error in the pressure due to differences in  $T$  are  $\sim \Delta T/2T$  or about 5% or less.

## Results

Figure 1 shows representative Si2p and O1s XPS spectra acquired at 1.5 torr of water vapour and at temperatures: 23C, -6C and -15C, corresponding to RH ~5%, 50% and 100% RH respectively. The dry silicon oxide (RH ~5%) showed an O1s peak at 532.3 eV and Si2p peaks at 99.4 and 103.4 eV (fig. 1a), corresponding to  $\text{Si}^0$  and  $\text{Si}^{4+}$  oxidation states respectively. Some residual intensity between these two peaks indicates the presence of small amounts of material with sub-oxide stoichiometry (less than 10% of the  $\text{Si}^{4+}$  peak intensity).<sup>20</sup> The suboxide intensity can be fitted mainly by two peaks for the  $\text{Si}^{1+}$  and  $\text{Si}^{3+}$  oxidation states and by small amounts of  $\text{Si}^{2+}$ , as already observed in XPS studies on oxide growth on a Si(111) substrate.<sup>31</sup> As water adsorbs on the surface a new peak appears in the O1s region (figure 1 b). For humidity of 100% and above a microscopic liquid or ice layer depending on the temperature could be seen by the naked eye. No peak is observed in the Si2p region in these conditions. In the O1s region only gas phase and adsorbed water peaks at 535.0 and 533.7 eV are observed.

In figure 2a we show the water film thickness determined from the XPS peak intensities as a function of RH at a constant 1.5 torr water vapor pressure measured on 3 different samples. The three samples showed similar level of C contamination ( $\sim 1/10$  of a monolayer). In figure 2b we show the water film thickness as a function of RH of three experiments performed at isobaric conditions of 1.5, 3 and 4 torr.

The fact that the three results collapse into one and the same curve indicates that the approximation of relative humidity described above is indeed very good. In figure 2c we show the results from two samples with  $\sim 1/2$  monolayer and  $\sim 1/10$  of a monolayer of C contamination. It can be observed that the sample with the higher contamination levels shows a lower water film thickness at the middle humidity range. However, this difference is less than one water monolayer.

In figure 3 (left axis) we show the water film thickness as a function of RH for many experiments, with different symbols corresponding to different samples and/or at different background water vapor pressures. As shown in the figure the water coverage increased rapidly with humidity to a thickness of  $\sim 0.6$  nm, or about 2 layers (assuming 0.3 nm per layer) at about 15% RH. After that it increased slowly, reaching 1.3 nm or  $\sim 4$  layers at  $\sim 75\%$  RH. Above 75% RH the coverage increased rapidly and at 100% RH a macroscopic drop, visible through the viewport, was formed. These results agree with previous measurements by other authors using different techniques.<sup>15,16</sup>

AFM images were acquired as the RH increased from  $\sim 5\%$  to 90%. The topographic SPFM images showed a flat surface, within 0.3 nm, at any humidity, indicating that the adsorbed water film is flat and homogenous. Changes in the surface potential  $\Delta\Phi$  were measured using the AFM in the Kelvin Probe mode. The surface potential was uniform across the SiO<sub>2</sub> surface and increased always with RH saturating at 75% RH. The results are plotted in figure 3 (right axis) together with the XPS thickness measurements (left axis). As can be seen, the surface potential starts to change at  $\sim 20\%$  RH, above which it increases rapidly until it saturates at 75% RH at 400 mV. In some experiments a lower saturation value was obtained, a variability that we attribute to contamination. The shape of the curve however was always the same. The increase in surface potential indicates the formation of a net positive charge or dipole on the surface.

To obtain information on the bonding structure of water we performed NEXAFS experiments at the O K-edge. The resulting spectra for 70% RH are shown in the bottom panel of figure 4. These spectra were measured at three different temperatures (-9, -4 and +1°C) at 70% RH, where the water film thickness is about 5 molecular layers. The spectra showed remarkable differences with temperatures that

we will discuss in the next section. Spectra taken for films with thickness  $< 5$  molecular layers (i.e. taken at  $\text{RH} < 70\%$ ) were too noisy to extract conclusions from their shape and are not shown here. A small peak around 532 eV was often observed that is associated with oxygen containing carbon contaminants.

## Discussion

Unfortunately the small binding energy differences and broad peaks of the surface species containing oxygen ( $\text{SiO}_2$ , OH and  $\text{H}_2\text{O}$ ) prevents us from actually detecting the silanol groups that we believe are present on the surface. It has been predicted theoretically<sup>10</sup> and shown experimentally<sup>14</sup> that on a silanol-rich surface water adsorbs forming a completely H-bonded structure in the first monolayer. Laser-induced thermal desorption experiments have shown that in a fully hydroxylated  $\text{SiO}_2$  surface  $\sim 70\%$  of the silanol groups are H-bonded.<sup>32</sup> Our surface potential measurements (figure 3) show that up to  $\sim 20\%$  RH the surface potential does not change appreciably, suggesting that for the first 1 to 2 monolayers the water molecules adsorb with their dipole moment either parallel to the surface or randomly oriented, in line with theoretical predictions.<sup>11</sup> At higher humidity, when 2 or more water layers are adsorbed, the average dipolar orientation changes and points towards the gas phase. After 4-5 layers the average dipolar orientation is no longer changing, which indicates that the bonding structure of water has reached the final value adopted by the thick film.

NEXAFS provides information on the local electronic structure of a given species, oxygen in the present case, and is particularly sensitive to the H-bonding environment of the molecule. It is for that reason that it has been extensively used in studies of water<sup>35</sup>. Its local character means that the first neighboring shell of molecules contributes the most to the spectrum.

When considering water films only a few molecules thick it is clear that the “solid” or “liquid” nomenclature might not be strictly appropriate as these refer to phases of water defined by bonding and ordering extending to many neighbors. We therefore use the terms “ice-like” and “liquid-like” to indicate a bonding configuration where the first shell of neighbor molecules is fully H-bonded to the



central molecule or not. The surface spectra of macroscopic ice and liquid water shown at the top of figure 4 (reprinted from Ref. 34) are characterized by peaks labeled A, B and C at 535, 537 and 542 eV respectively. Calculations have shown<sup>35</sup> that these features are due to water molecules with dangling H-bonds (peak A), and to double donor H-bonded molecules (B, C). Peak A is present in all phases because the surface contains necessarily dangling H-bonds. The bulk phase of liquid contains additional broken H-bonds that increase the intensity of peak A relative to ice. For the present analysis therefore it is the relative intensity of peaks B and C that is most informative. Fully coordinated water molecules contribute more strongly to peak C which, as shown in the figure, introduces characteristic differences in the spectra of ice and liquid. The solid or liquid character of our water film can thus be judged from the degree of H-bonding coordination per molecule manifested in the spectra shown in the bottom panel of figure 4. The spectrum for the film at -9 °C shows a shape very similar to that of bulk ice at -10 °C. On the other hand the film formed at +1 °C shows a shape that is similar to that of the bulk liquid. At -4 °C the character of the film is intermediate between liquid and ice, which might correspond to an ice-like bilayer near the surface in contact with a liquid-like layer on top.<sup>34</sup> In an attempt for a more quantitative analysis we fit the main features of the spectra with Gaussian peaks centered at the positions of the known A, B and C peaks, as shown in figure 4. Although this is clearly a simplification, the ratio of the areas of peaks C and B can then be used to compare different spectra. The obtained ratios are shown in Table I. Bulk water shows a C/B ratio close to 2 while in ice this ratio raises to 3.5. For the water films, the spectra obtained above 0°C show a C/B ratio of 1.8, which is close to that in the bulk liquid. For the films at -9 °C the ratio is 3.2 ratio, close to that of ice.

Using infrared spectroscopy, Asay et al.<sup>15</sup> concluded that up to 4-5 monolayer the water film is more structured than the liquid, or “ice-like”. From our surface potential measurements we conclude that in this initial film the water molecules have a preferential orientation induced by the substrate. These structural differences might indicate adsorption energies slightly stronger than the sublimation energy of ice. Sneha et al.<sup>37</sup> performed laser-induced thermal desorption on a SiO<sub>2</sub> films grown on Si(100). The

experimental set-up was similar to our XPS experiment. They found that the desorption activation energy decreased from 20 kcal mol<sup>-1</sup> to 12 kcal mol<sup>-1</sup> with coverage. The higher energy stabilizes water condensation at 0.3 ML coverage, where 1 ML corresponds to one water molecule adsorbed per silanol group. The SiO<sub>2</sub> surface was considered to be fully hydroxylated with a silanol group density of  $4.6 \pm 0.4 \times 10^{14}$  cm<sup>-2</sup>. From the different pressure and temperature conditions in these experiments we conclude that the 0.3 ML coverage was reached at 15% RH. In our measurements 15% RH corresponds to the completion of 1-2 monolayer, just before the potential of the surface starts to increase. So this corresponds probably to the structured first water monolayer already reported<sup>14</sup>. Above 0.3 ML (or 15 % RH) the desorption energy was found to be 12.8 kcal mol<sup>-1</sup> with zero order kinetics and with parameters very similar to those from ice sublimation. These results indicate that the difference in water desorption energy for films higher than 1 monolayer (i.e., above 15% RH) must be very small.

## Conclusions

In summary, we have performed studies of the growth of water on SiO<sub>2</sub> films on Si(111) wafers as a function of RH both in air-vapor mixtures and in pure vapor environments. We have determined the film thickness using XPS and found that at ~15% RH the surface is covered by a water film about 2 monolayers thick. This film does not change the surface potential of the surface, indicating a parallel or random orientation of the dipole moment of the molecules. Between 15-75% RH there is a slowdown in the rate of adsorption while 2-3 additional water layers are adsorbed. Most of the surface potential increase occurs in this regime, with a positive value that reflects the formation of a dipole-oriented water layer as found at the surface of bulk water. The NEXAFS results also indicate that in films thicker than 4-5 monolayers the local electronic structure of the water molecules is similar to that of the bulk liquid above 0°C, and similar to that of ice below that temperature. Only within a few degrees from zero the spectrum resembles that of a mixture of liquid and ice.

## **Acknowledgments**

This work was supported by the Director, Office of Energy Research, Basic Energy Sciences, Materials Sciences Division, and in part also by the Division of Chemical Sciences, Geosciences, and Biosciences of the U.S. Department of Energy under Contract No. DE-AC02-05CH11231. AV acknowledges financial support from DURSI/AGAUR, Generalitat de Catalunya and the Ramon y Cajal Program of the Ministerio de Educación y Ciencia, Spain. GK thanks the Alexander-von-Humboldt foundation for financial support.

## **Supporting Information**

Energy calibration and background subtraction procedures in the O K-edge NEXAFS measurements are provided as supporting information. This information is available free of charge via the Internet at <http://pubs.acs.org>.

FIGURES and CAPTIONS:

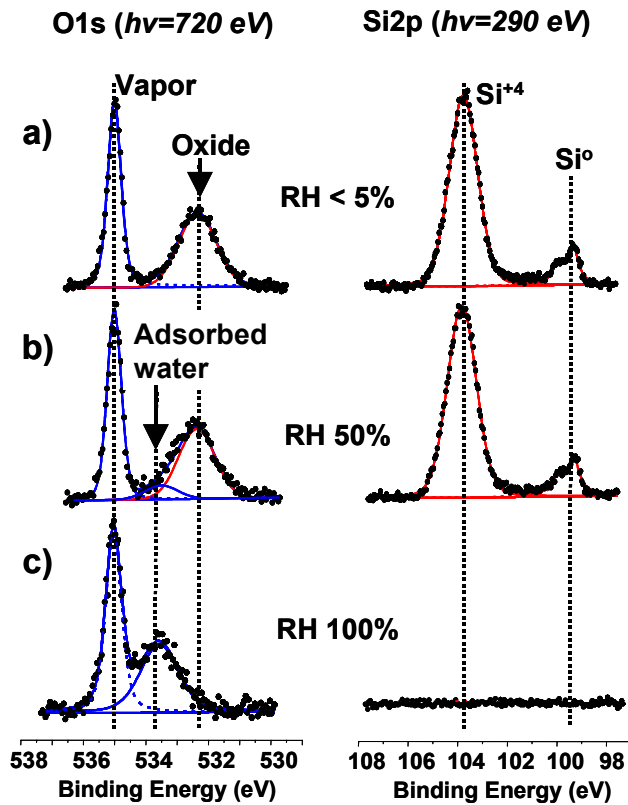


**Figure 1:** O1s and Si2p XPS spectra of the SiO<sub>2</sub>/Si(111) wafer under 1.5 torr of water: (a) dry conditions ( $T = 23$  °C, RH~5%). (b)  $T = -6$  °C (~50% RH), which produces a water film about 3 layers thick on the surface. (c)  $T = -15$  °C (100% RH), with a macroscopic ice layer condensed on the surface.

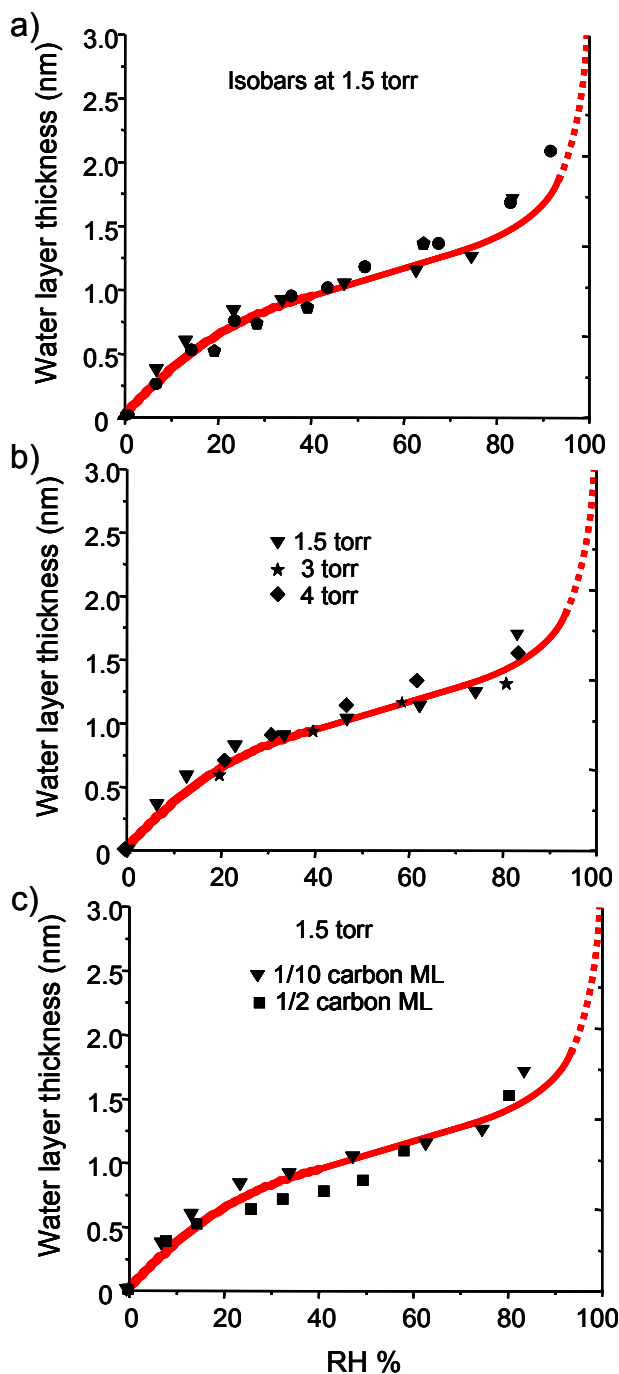


**Figure 2:** a) Water film thickness as a function of relative humidity (RH) as determined from the XPS measurements. Isobaric experiments were performed at constant 1.5 torr of water vapor pressure and varying sample temperature to change RH at sample surface. Different symbols correspond to experiments performed on different samples. b) Water film thickness as a function of RH from three isobaric experiments at three different water vapor pressures. When plotted as a function of RH with the saturation pressure corresponding to the substrate temperature the three sets of data collapse into the same curve. c) Influence of carbon contamination. The water film thickness as a function of RH of the

sample with the lowest contamination ( $1/10$  of a monolayer) is compared with that of a more contaminated sample ( $1/2$  of a monolayer). The water film thickness is slightly higher for the cleaner sample at middle range RH.

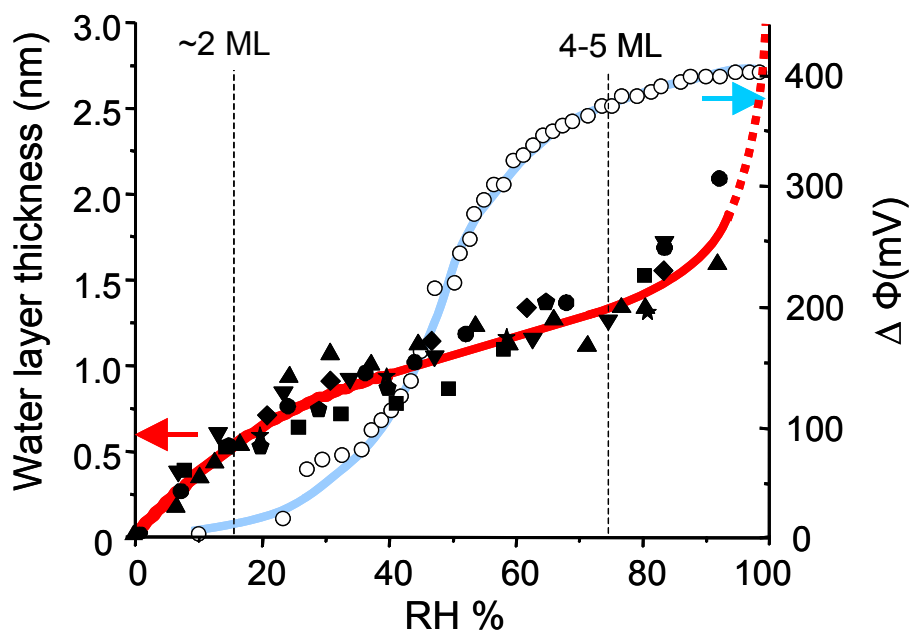
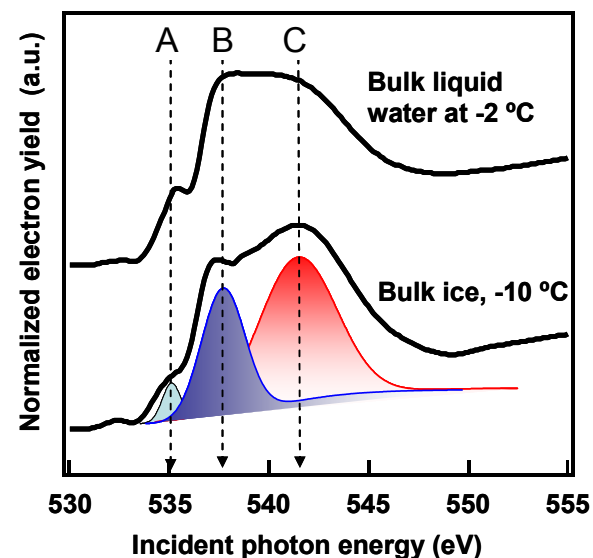


**Figure 3:** Left y-axis (solid symbols): Water film thickness as a function of relative humidity (RH) as determined from the XPS measurements. Different symbols correspond to experiments performed on different samples and/or at different background water vapor pressures. The thickness of 0.3 nm is assumed to correspond to one molecular layer. Right y-axis (open symbols): Changes in surface potential as a function of RH measured by the AFM in a different chamber, operating in the Kelvin probe mode at 21 °C.



~5-6 monolayer water film on SiO<sub>2</sub>

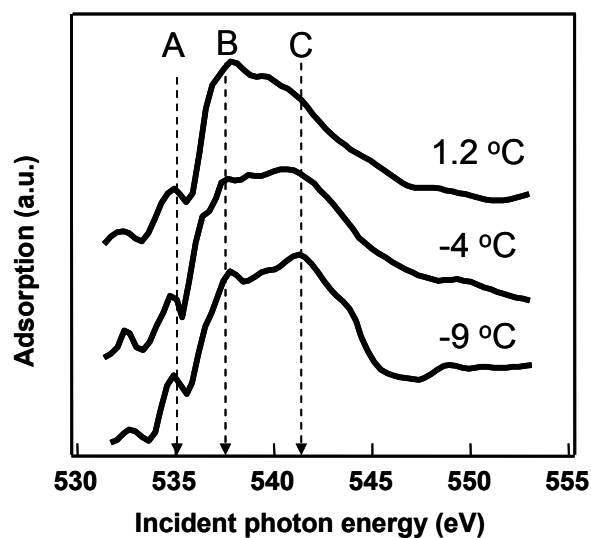


**Figure 4:** Top: NEXAFS spectra of ice and bulk super-cooled liquid water (from Ref. 34). The spectra show three peaks at 535 eV, 537 eV and 542 eV (*A*, *B* and *C* respectively). Peaks *A* and *B* show more intensity for bulk water while peak *C* is substantially more intense for ice. Bottom: NEXAFS spectra of 4-6 monolayer thick water films on SiO<sub>2</sub>. The three spectra were acquired at the same relative humidity of ~70%, but at different pressures/temperatures. The spectrum taken at 1.2°C shows a liquid-like shape, while the spectrum taken at -9°C shows a clear ice-like shape. A simple fitting using Gaussian peaks for *A*, *B* and *C* peaks is showed for the bulk ice spectrum.



|                | Bulk liquid water at <b>-2 °C</b> | Bulk ice at <b>-11 °C</b> | 4-6 monolayer water film on SiO <sub>2</sub> at <b>1.2 °C</b> | 4-6 monolayer water film on SiO <sub>2</sub> at <b>-4 °C</b> | 4-6 monolayer water film on SiO <sub>2</sub> at <b>-9 °C</b> |
|----------------|-----------------------------------|---------------------------|---|--|--|
| C/B peak ratio | <b>2.2</b>                        | <b>3.5</b>                | <b>1.9</b>  | <b>2.8</b>   | <b>3.2</b>   |

**Table I:** Ratio of the areas of Gaussian curves fitting peaks C and B in the NEXAFS of figure 3.

## REFERENCES

- 1 Thiel, P.A.; Madey, T.E. *Surf. Sci. Rep.* **1987**, 7, 211.
- 2 Henderson, M.A. *Surf. Sci. Rep.* **2002**, 46, 1.
- 3 Ewing, G.E. *J. Phys. Chem. B* **2004**, 108, 15953.
- 4 Verdaguer, A.; Sacha, G.M.; Bluhm, H.; Salmeron, M. *Chem. Rev.* **2006**,
- 5 Al-Abadleh, H.A.; Grassian, V.H. *Surf. Sci. Rep.* **2003**, 52, 63.
- 6 R.K. Iler Ed. *The Chemistry of Silica*; Wiley: New York, 1979.
- 7 Vansant, E.F.; Van Der Voort, P. and Vrancken, K.C *Studies in Surfaces Science and Catalysis vol 93: Characterization and Chemical Modification of the Silica Surface*; Elsevier B.V.: Amsterdam , 1995.
- 8 A.P. Legrand Ed. *The Surface Properties of Silica*; Wiley: New York, 1998.
- 9 Chuang, I-S. and Maciel, G.E. *J. Phys. Chem. B* **1997**, 101, 3052.
- 10 Yang, J.; Meng, S.; Xu, L.F.; Wang, E.G. *Phys. Rev. Lett.* **2004**, 92, 146102.
- 11 Yang, J.; Meng, S.; Xu, L.F.; Wang, E.G. *Phys. Rev. B.* **2005**, 71, 035413.
- 12 Lu, Z.-Y.; Sun, Z.-Y.; Li, Z.-S.; An, L.J. *J. Phys. Chem. B* **2005**, 109, 5678.
- 13 Yang, J.; Wang, E.G. *Phys. Rev. B.* **2006**, 73, 035406.
- 14 Aarts, I.M.P.; Pipino, A.C.R.; Hoefnagels, J.P.M.; Kessels, W.M.M.; van de Sanden, M.C.M. *Phys. Rev. Lett.* **2005**, 95, 166104.
- 15 Asay, D.B. and Kim, S.H. *J. Phys. Chem. B* **2005**, 109, 16760.
- 16 Sumner, A.L.; Menke, E.J.; Dubowski, Y.; Newberg, J.T.; Penner, R.M.; Hemminger, J.C.; Wingen, L.M.; Brauers, T.; Finlayson-Pitts, B. *Phys. Chem. Chem. Phys.* **2004**, 6, 604.
- 17 Du, Q.; Freysz, E.; Shen, Y.R. *Phys. Rev. Lett.* **1994**, 72, 238.
- 18 Ostroverkhov, V.; Glenn, A.; Waychunas, G.; Shen, Y.R. *Phys. Rev. Lett.* **2005**, 94, 046102.
- 19 W. Kern, Ed. *Handbook of Semiconductor Cleaning Technology*; Noyes Publishing: Park Ridge,NJ, 1993.
- 20 Fukano, A.; Oyanagi, H. *J. Apl. Phys.* **2003**, 94, 3345
- 21 Seah, M.P.; Spencer, S.J. *J. Vac. Sci. Technol.* **2003**, 21, 345.
- 22 Bluhm, H.;Pan, S.H.; Xu, L.; Inoue, T.; Ogletree, D.F.; Salmeron, M. *Rev. Sci. Instrum.* **1998**, 69, 1781.
- 23 RHK Technology, Inc. Troy. MI USA
- 24 Hu, J.; Xiao, X.-D.; Ogletree, D.F.; Salmeron, M. *Appl. Phys. Lett.* **1995**, 67, 476.
- 25 Verdaguer A., Sacha G.M., Luna M., Ogletree F.D., Salmeron M. *J. Chem. Phys.* **2005**, 123, 124703.

- 26 Ogletree F.D.; Bluhm, H.; Lebedev, G.; Fadley, C.S.; Hussain Z.; Salmeron M. *Rev. Sci. Instrum.* **2002**, *73*, 3872.
- 27 SPECS Phoibos 150 hemispherical analyzer, Specs GmbH, Berlin, Germany.
- 28 S. Hüfner Ed., *Photoelectron Spectroscopy*, 3rd Ed.; Springer: Berlin, 2003.
- 29 Yeh, J.J.; and Lindau, I. *At. Data Nucl. Data Tables* **1985**, *32*, 1.
- 30 Himpsel, F.J.; Mcfeely, F.R.; Taleb-Ibrahimi, A; Yarmoff, J.A. *Phys. Rev. B* **1988**, *38*, 6084.
- 31 The mean free path of the photoelectrons is calculated using the relations for oxides in: Seah, M. P.; Dench, W. A. *Surf. Interface Anal.* **1979**, *1*, 2
- 32 Keister, J.W.; Rowe, J.E.; Kolodziej, J.J.; Niimi, H.; Tao, H.-S.; Madley, T.E.; Lucovsky, G. *J. Vac. Sci. Technol. A* **1999**, *17*, 1250.
- 33 Sneh, O.; Cameron, M.A. and George S.M. *Surf. Sci.* **1996**, *364*, 61.
- 34 Bluhm, H.; Ogletree, D.F.; Fadley, Ch. S.; Hussain, Z.; Salmeron, M. *J. Phys.: Condens. Matt.* **2002**, *14*, L227.
- 35 Myneni, S.; Luo, Y.; Näslund, L. Å.; Cavalleri, M.; Ojamäe, L.; Ogasawara, H.; Pelmenchikov, A.; Wernet, Ph.; Väterlein, P.; Heske, C.; Hussain, Z.; Petterson, L.G.M. and Nilsson, A. *J. Phys.: Condens. Matt.* **2002**, *14*, L213.
- 36 Marcelli, A.; Davoli, A.; Biaconi, A.; Garcia, J.; Gargano, A.; Natoli, C.R.; Benfatto, M. Chiaradia, P.; Fantoni, M.; Fritsch, E.; Calas, C.; Petiau, J. *J. Phys. (Paris) Colloq.* **1985**, *46*, C-8, 107.
- 37 Sneh, O., Cameron, M.A. and George, S.M. *Surf. Sci.* **1996**, *364*, 61.